*Int. J. Therm. Sci.* (2001) 40, 927–936

S1290-0729(01)01279-0/FLA

# Experiments and modelling of natural gas combustion ignited by a pilot diesel fuel spray

Makame Mbarawa [a*], Brain Edward Milton [b], Robert Thomas Casey [b]

[a] *Department of Mechanical Engineering, Technikon Pretoria, Private Bag X680, Pretoria 0001, South Africa*

[b] *School of Mechanical and Manufacturing Engineering, University of NSW, Sydney, NSW 2052, Australia*

(Received 23 July 1999, accepted 19 December 2000)

**Abstract** — Experiments and numerical simulations have been carried out in order to understand the combustion of natural gas (NG) under diesel cycle conditions. The study used a natural gas/air mixture with a pilot diesel fuel spray for ignition in a constant volume combustion chamber. The experiments were carried out under conditions as close as possible to those existing in a gas engine operating according to a diesel cycle. A three-dimensional (3D) numerical model incorporating complex interaction between the fuels during combustion was used. Simulation results compare well with the experiments. It was shown that NG combustion in diesel environments can be improved by using an injector with a great number of small holes and by increasing the injection pressure of the pilot diesel fuel, in this case to about 60 MPa. © 2001 Éditions scientifiques et médicales Elsevier SAS

**alternative fuels / diesel engine / dual-fuelling / natural gas / numerical modelling**

## Nomenclature

| | | |
|---|---|---|
| $a_i$ | finite-difference coefficients | |
| $A_A$ | pre-exponential factor | $m^3{\cdot}kg^{-1}{\cdot}s^{-1}$ |
| $A_{eff}$ | effective area | $m^2$ |
| $C_d$ | discharge coefficient | |
| $C_R$ | reaction spread factor | |
| $D$ | diffusion flow rate | $kg{\cdot}s^{-1}$ |
| $E_A$ | activation energy | $kJ{\cdot}mol^{-1}$ |
| $F$ | convection flow rate | $kg{\cdot}s^{-1}$ |
| $m$ | mass | kg |
| $P$ | pressure | kPa |
| $P_{ng,o}$ | stagnation pressure of natural gas | kPa |
| $R_m$ | fuel reaction rate in multi-fuel | $kg{\cdot}m^{-3}{\cdot}s^{-1}$ |
| $R_s$ | fuel reaction rate in single fuel | $kg{\cdot}m^{-3}{\cdot}s^{-1}$ |
| $R_{ng}$ | gas constant of natural gas | $kJ{\cdot}mole^{-1}{\cdot}K^{-1}$ |
| $R_u$ | universal gas constant | $kJ{\cdot}mole^{-1}{\cdot}K^{-1}$ |
| $S_c$ | linearised source term | |
| $S_\phi$ | source term in the model | |
| $T$ | temperature | °C |
| $T_{ng}$ | temperature of natural gas | °C |
| $T_{ng,o}$ | stagnation temperature of natural gas | °C |
| $t$ | time | ms |
| $X$ | mass fraction | |
| $V_{ng}$ | injection velocity of natural gas | $m{\cdot}s^{-1}$ |
| $U_r, U_\theta, U_z$ | velocity | $m{\cdot}s^{-1}$ |
| $Z_{ng}$ | natural gas compressibility factor | |

*Greeks letters*

| | | |
|---|---|---|
| $\phi$ | dependent variable | |
| $\gamma_{ng}$ | specific heat ratio of natural gas | |
| $\Gamma_\phi$ | eddy diffusivity | $kg{\cdot}m^{-1}{\cdot}s^{-1}$ |
| $\rho$ | density | $kg{\cdot}m^{-3}$ |

*Subscripts*

| | |
|---|---|
| c | point indicator |
| E,W,N,S,T,B | face indicators |
| f | fuel |
| g | gaseous charge |
| ng | natural gas |
| m | mixture |
| $O_2$ | oxygen |
| 0 | stagnation value |
| s | single fuel |
| $r, \theta, z$ | cylindrical co-ordinates |

* Correspondence and reprints.
*E-mail address:* MMbarawa@techpta.ac.za (M. Mbarawa).

## 1. INTRODUCTION

A shortage of crude oil is expected during the early decades of this century. In addition, air pollution is becoming more serious and tighter regulation of both 'local' and 'global' emissions from engines is anticipated. This has resulted in an increased interest to use natural gas (NG) as fuel for internal combustion engines. Natural gas resources are vast, are widespread geographically and are not limited to politically sensitive locations as is typical for crude oil. Based on current consumption rates, the estimated total, recoverable gas, including proven reserves, is adequate for almost 200 years [1]. To benefit from the use of natural gas in internal combustion engines, it is necessary to understand its combustion under the appropriate conditions and to study the effects of various parameters on it.

Natural gas combustion is characterised by a long ignition time delay [2–5] and cannot be used directly as a fuel for an internal combustion engine using compression ignition (that is, working on a diesel cycle). Hence some type of ignition aid is required. Dual fuelling (DF), is one practical way to use natural gas in such an engine. In this approach, NG and air are inducted into the engine cylinder and the mixture is then ignited by a pilot diesel fuel spray directly into the combustion chamber. The inclusion of natural gas with the air modifies the initial combustion process of the pilot fuel spray which is acting as the source of ignition. Although many studies have been reported on the performance and emissions of dual-fuel engines [2–10], the complex DF combustion processes mechanisms which involve the modified ignition delay, diffusion burning, flame propagation and possible flame quench are unclear. The objective of the present work is to study, at a fundamental level, these combustion processes.

## 2. EXPERIMENTAL SETUP AND PROCEDURES

A cylindrical, constant volume combustion bomb (CVCB) was designed, in order to simulate in a basic apparatus the conditions of high temperature and pressure in diesel engines at the end of the compression stroke. It allowed convenient observation of the combustion of the pre-mixed natural gas–air mixture ignited by pilot fuel injection. It is electrically heated and is pressurised so that the pre-ignition conditions can be obtained in quiescent conditions for its natural gas–air mixture. Its dimensions are 108 mm bore and 30 mm depth. *Figure 1* shows the construction of the CVCB. A single shot diesel injection system was developed from an in-line fuel injection pump giving characteristics identical to those in a diesel engine injection system. A needle type injector with four holes was mounted vertically on the centre of the upper face with the spray from each orifice oriented with an angle of 15° downwards relative to the horizontal. The injection pressure and the needle lift signal were measured to determine the injection conditions. The temperature, which varies with location and time, and the instantaneous pressure which is uniform at any instant in the chamber were measured, respectively, with a thermocouple (type K, 2 mm diameter) and a water-cooled piezoelectric transducer. The thermocouple was mounted at the mid-radius on the upper face giving an approximate, average temperature. Acquisition and processing of these signals were carried out on a computer.

The test conditions used in the CVCB are summarised below:

Initial temperature: 580–950 K.

Initial pressure: 1.5–4.5 MPa.

Four-hole injector: 0.2 mm diameter per hole.

Pre-set injector pressure: 20 MPa.

Diesel mass injected: 27–57 mg.

An illustration of the full CVCB set up is shown in *figure 2*. A more detailed description of the experiment and of the procedures has been given by Mbarawa [11].

## 3. NUMERICAL MODEL

### 3.1. Model description

A simplified 3D, finite volume model [12] has been developed for simulation of the DF combustion in the cylindrical constant volume combustion bomb. The model incorporates the main processes taking place in the chamber, i.e., fuel spray development, spray impingement on the wall, droplet evaporation, heat transfer and combustion which include the complex interaction between the fuels. The NG may be incorporated into the system either pre-mixed with air or injected in a separate spray near to the diesel injector. In this study, only the DF combustion with pre-mixed NG is reported. The diesel fuel is simulated in a similar although simplified manner to that of a normal diesel engine.

In the formulation, a cylindrical co-ordinate $(r, \theta, u)$ system has been employed in which velocity components are denoted by $(U_r, U_\theta, U_z)$. The turbulence model is

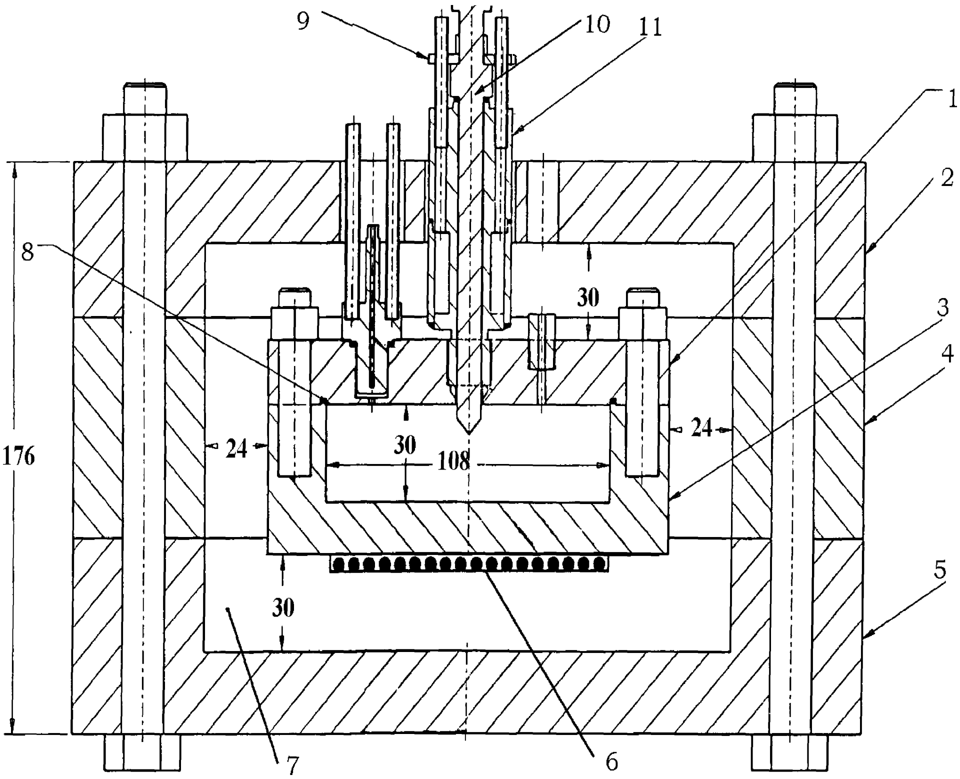


**Figure 1.** Dual-fuel constant volume combustion bomb: (1) cylinder head; (2) top outer casing; (3) combustion chamber; (4) middle inner casing; (5) bottom outer casing; (6) heating element; (7) insulation blanket; (8) copper ring; (9) injector clamp; (10) injector; (11) water-cooled injector holder.

described by means of the $\kappa$–$\varepsilon$ eddy diffusivity model of Launder and Spalding [13]. The governing equation consists of equations for continuity, momentum and energy in cylindrical co-ordinate expressed in general form as follows:

$$\frac{\partial(\rho_g\phi)}{\partial t}+\frac{1}{r}\frac{\partial(\rho_g r U_r\phi)}{\partial r}+\frac{1}{r}\frac{\partial(\rho_g U_\theta\phi)}{\partial\theta}+\frac{\partial(\rho_g U_z\phi)}{\partial z}$$
$$-\frac{1}{r}\frac{\partial}{\partial r}\left(r\Gamma_\phi\frac{\partial\phi}{\partial r}\right)-\frac{1}{r}\frac{\partial}{\partial\theta}\left(\frac{\Gamma_\phi}{r}\frac{\partial\phi}{\partial\theta}\right)$$
$$-\frac{\partial}{\partial z}\left(\Gamma_\phi\frac{\partial\phi}{\partial z}\right)=S_\phi \tag{1}$$

where:

- ($\phi$) represents the dependent variables which denote either the mass fractions of the chemical species, the specific enthalpy or the momentum ($U_r$, $U_\theta$, $U_z$) due the distillate evaporation as required;
- $\Gamma_\phi$ is the effective diffusity;
- $S_\phi$ is the source term;
- $\rho$ is the density.

In reality, diesel fuel consists of many different components. However, because the diesel fuel in this dual-fuelling application supplies only a small proportion of the overall energy, it is, for simplification, considered here only as a single substance $C_{12}H_{26}$. This provides an approximate, average value of its properties. In this model, 16 chemical species are considered. They are diesel vapour ($C_{12}H_{26}$), the NG fuel components ($CH_4$, $C_2H_6$, $C_3H_8$), 12 dissociated species of air, NG and combustion products, H, O, N, $H_2$, OH, CO, NO, $O_2$, $H_2O$, $CO_2$, $H_2$, and $N_2$.

### 3.2. Solution of the partial differential equation

In the current model, equation (1) is discretised by using a control volume, finite difference method as suggested by Patankar [14]. The equation for $\phi$ can then be expressed as follows:

$$a_c\phi_c = a_W\phi_W + a_E\phi_E + a_N\phi_N + a_S\phi_S + a_T\phi_T + a_B\phi_B + s_c \tag{2}$$

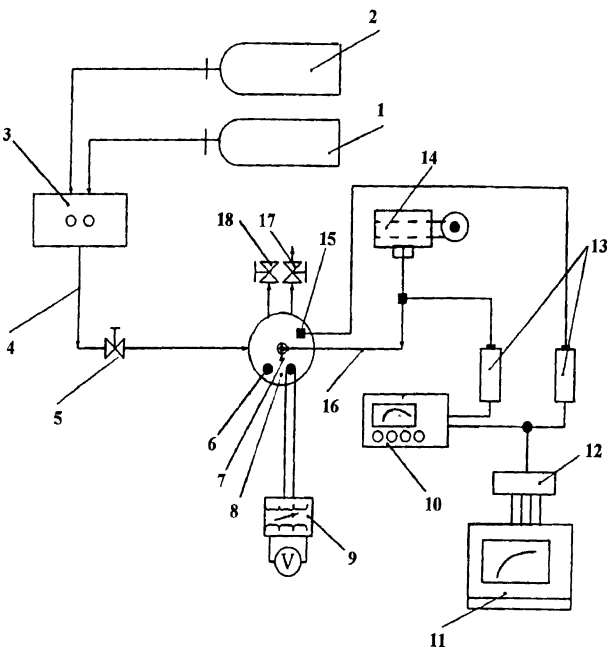


**Figure 2.** Experimental set-up: (1) compressed air; (2) compressed gaseous fuel; (3) control panel; (4) air–gas line; (5) inlet valve; (6) thermocouple; (7) water cooled injector; (8) constant volume combustion bomb (CVCB); (9) heater power supply control; (10) oscilloscope; (11) PC; (12) data acquisition; (13) charge amplifier; (14) fuel pump; (15) pressure transducer; (16) fuel line; (17) outlet valve; (18) safety valve.

where, $a_i$ $(i = \mathrm{E, W, N, S, T, B})$ are finite difference coefficients around the point. The convection–diffusion flux is evaluated using the power-law scheme.

$$a_i = D_i\left[0, \left(1 - 0.1\left|\frac{F_i}{D_i}\right|\right)^5\right] + [0, -F_i] \qquad (3)$$

where, $F$ is convection flow rate and $D$ is the diffusion flow rate.

### 3.3. Computational method

A finite-difference equation for each cell derived from equation (2) is solved implicitly in terms of time and space. All unknown variables at the next time step in every grid point are obtained by a Gauss–Seidel iteration [14]. The source or sink terms required in the model are obtained from the sub-models of the pilot distillate injection, dual-fuel combustion and heat transfer as described below.

The injector with its four equally spaced-holes is centred in the combustion chamber enabling the computation to be confined to one quarter of the chamber. For this, the computational domain consisted of a single sector with 40 radial grid points, 44 in the azimuthal direction and 24 in the axial direction. Before the computational calculations were performed, a convergence grid study was undertaken, details of which are provided in Mbarawa [11].

### 3.4. Sub-models

Many sub-models were required but only the most significant will be discussed here.

#### 3.4.1. Diesel fuel injection and its trajectory

The approach, developed by Hiroyasu and Nishida [15], was used for the fuel flow rate and spray penetration. The spray was assumed to be conical, divided arbitrarily into many 3D parcels. The spray cone was segmented at every calculation time step in the spray growth direction (L), into 3 layers in the radial (M) direction and 8 divisions in the circumferential (N) direction. The radial layer division in the N direction was staggered. The evaporation process was modelled from a quasi-steady analysis of a single droplet based on its heat and mass transfer. Spray parcels reaching the wall were assumed to move radially along it from the impingement. The droplets in each spray parcel were assumed to be spherical with identical size, velocity and properties.

#### 3.4.2. Mixed burning of diesel fuel and natural gas

Chemical reaction schemes are available for simple hydrocarbons but these are not readily applicable to 3D modelling of either diesel or dual-fuel combustion. The basic model used is that given by Westbrook and Dryer [16]. That is, a simple global model, equation (4) of the fuel burning rate has been adopted.

$$R_\mathrm{S} = -A_\mathrm{A}\rho_\mathrm{g}^{a+b} X_\mathrm{f}^a X_{\mathrm{O}_2}^b \exp\left(\frac{-E_\mathrm{A}}{R_\mathrm{u} T_\mathrm{g}}\right) \qquad (4)$$

Values for the various constants ($A_\mathrm{A}$, $a$, $b$, and $E_\mathrm{A}$) appropriate to the present study are given in *table I*.

The single fuel reaction rate of equation (4) considers only one fuel and the oxygen mass fractions. In the case of dual-fuel combustion, several fuel species react simultaneously modifying the diesel fuel combustion which is providing the ignition. All these fuel species are involved in the oxygen reaction and will interact to stimulate the chain reactions of others. Hence, a "reaction

TABLE I
Data for combustion calculations: constants for single-fuel reaction rates.

| Fuel type | $A_A$ ($m^3 \cdot kg^{-1} \cdot s^{-1}$) | $a$ | $b3$ | $E$, $kJ \cdot mol^{-1}$ |
|---|---|---|---|---|
| Diesel ($C_{12}H_{26}$) | $6.96 \times 10^6$ | 1.25 | 1.50 | 100 000 |
| Methane ($CH_4$) | $1.87 \times 10^8$ | 0.70 | 1.30 | 202 000 |
| Ethane ($C_2H_6$) | $8.11 \times 10^8$ | 1.10 | 1.65 | 125 000 |
| Propane ($C_3H_8$) | $6.16 \times 10^8$ | 1.10 | 1.65 | 125 00 |

spread factor” $C_R$, [12] was introduced to evaluate the effect of the individual fuel reaction rates on the multi-fuel combustion. It applies to each fuel component $i$, $i$ varying from 1 to $n$, where $n$ is the number of individual fuels. To understand this, assume that the reaction rate of each fuel parcel, which consists of one of the $n$ different fuels in the mixture, is $R_{mi}$, when burning in the presence of all the other fuels. If it is defined such that the total reaction rate of the mixture $R_m$ can be obtained by summing the individual values, then:

$$R_m = \sum_{i=1}^{n} R_{mi} \tag{5}$$

The value of $R_{mi}$ will not be identical to the reaction rate $R_{si}$ determined from equation (4) for the same fuel reacting alone at its appropriate mass fraction. To accommodate this difference, the presence of the other burning species is approximated by introducing the “reaction spread factor” which assumes that the principal modifying effect of the other fuels stems from their mass fractions. When applied to the global multi-fuel reaction, it gives:

$$R_m = R_{s,i} C_{R,i}^{a_i - 1}, \qquad C_{R,i} = \frac{\sum_{j=1}^{4} R_{s,j}}{R_{s,i}} \tag{6}$$

Consider the burning of diesel fuel in a NG/air mixture. If the NG proportions approach zero, all the fuel species other than those of the diesel fuel become negligible. The reaction spread factor for the diesel fuel becomes unity (equation (6)) and its reaction rate calculated by this method is identical to that of the diesel fuel from equation (4). The same argument applies to any of the other fuel species. However, when more than one fuel is in significant quantities, the reaction spread factor is not unity and the overall reaction rate from equation (6) is modified from that of equation (4).

Once an overall reaction rate has been determined, the procedure within the computational domain is relatively straightforward. That is, the temperature and hence the equilibrium combustion products can be calculated using well-known methods such as that of Olikara and Borman [17]. Subsequently, the heat release rate follows from the enthalpy difference of the products and reactions depending on their composition in each cell.

### 3.4.3. Pre-mixed NG addition

In the current research, only DF combustion with pre-mixed NG is being studied. However, in the original code, an injected NG option is available [18].

During the pre-mixed DF combustion studies, the mass of gaseous fuel can be determined simply from the ideal gas equation of state using the partial pressure of each constituent at the beginning of the test. This is because the pressure is low. In the case of DF combustion studies with injected NG, the NG injection rate was calculated from the isentropic, compressible, choked flow equation using a non-ideal gas equation (7). This is because the NG was injected under very high pressure into the chamber. The NG compressibility factor was determined by the Benedict–Webb–Rubin equation of state according to the mole fraction of its constituents. NG assumed to be 94.1% methane, 2.8% ethane, 0.1% propane, 1.5% carbon dioxide and 1.5% nitrogen. The mass injection rate of NG is calculated using:

$$\frac{dm_{ng}}{dt} = \frac{C_d A_{eff} P_{ng,o} \gamma_{ng}^{0.5}}{(Z_{ng} R_{ng} T_{ng,o})^{0.5}} \left( \frac{2}{\gamma_{ng} + 1} \right)^{(\gamma_{ng}+1)/(2(\gamma_{ng}-1))} \tag{7}$$

The injection velocity is assumed to be equal to the local speed of sound:

$$V_{ng} = (\gamma_{ng} Z_{ng} R_{ng} T_{ng,o})^{0.5} \tag{8}$$

## 4. RESULTS AND DISCUSSION

### 4.1. Model calibration against constant volume combustion bomb experiments

A number of dynamic pressure traces of combustion within the combustion bomb were obtained for a series of different initial conditions using both diesel fuel injected into air only and diesel fuel injected into an NG/air mixture. For comparative purposes, the numerical results were computed for the same initial conditions as those of the experiments.

Typical traces can be seen on *figure 3 (a)* and *(b)* for diesel fuel only and for pre-mixed NG DF combustion.

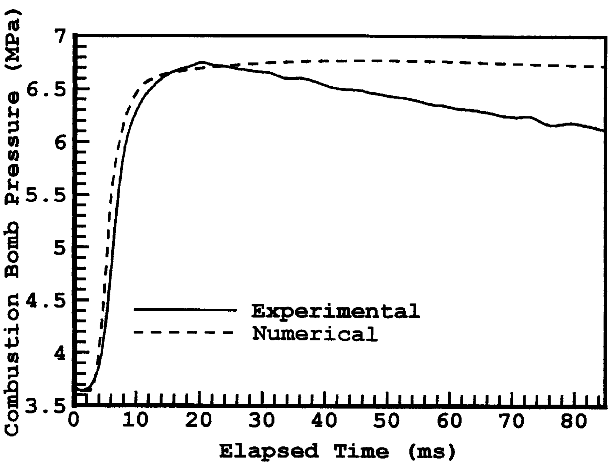


(a)

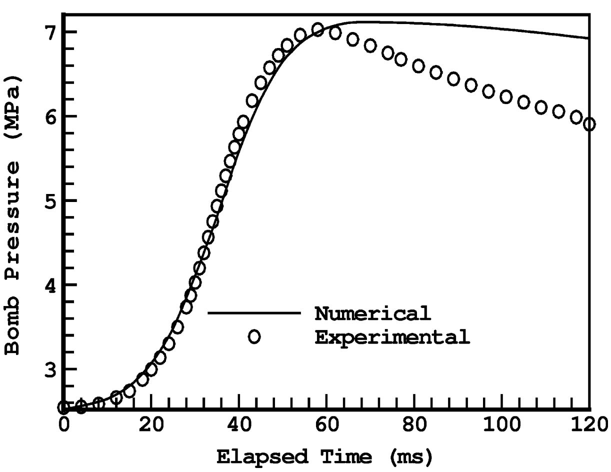


(b)

**Figure 3.** (a) Comparison of the calculated and measured bomb combustion pressure of diesel fuel combustion. Initial conditions: $P_0 = 3.65$ MPa, $T_0 = 773$ K, diesel injected: $m_{inj} = 55$ mg; (b) Comparison of the calculated and measured bomb combustion pressure of pre-mixed natural gas combustion. Initial conditions: $P_0 = 2.5$ MPa, $T_0 = 773$ K, diesel injected: $m_{inj} = 32.7$ mg, partial pressure of natural gas $= 0.13$ MPa.

These differ from traces obtained in engine tests due to the lower ignition conditions, the quiescent nature of the combustion and fact that no volume expansion occurs as the combustion progresses. The decay following the combustion peak is predominantly due to the heat transfer only in the numerics while in the experiments the time constant of the pressure transducer provides an additional effect. The numerical heat transfer model may require some improvement but the good agreement to the point of maximum pressure indicates that it is adequate. Some pressure leakage from the bomb may have occurred in the experiments but tests for this indicate that it is minimal.

Noticeable differences can be detected between the diesel and DF trace. Comparing the two, it can be seen that the typical pre-mixed DF trace has a longer ignition delay, reaches maximum pressure later and is a two stage process, where the burning begins slowly and then accelerates before slowing again in the final burnout. The acceleration in the combustion is where the natural gas conditions become such as to support a rapid flame development through the unburned mixture away from the spray zone. The diesel trace shows a short ignition delay followed by a sharp pressure rise with a shorter time to reach the maximum combustion pressure. Generally, the simulation results show good agreement in both cases of DF and diesel fuel combustion.

A further, parametric study using the numerical simulation was carried out to examine the effects of both pilot injection pressure and number of nozzle holes on the combustion of the pre-mixed natural gas–air mixture. For this study, the dimensions of the combustion chamber for the numerical analysis were taken as being identical to those of the experimental constant volume combustion bomb but the other parameters, such as air charge temperature, pressure and diesel injection pressure were simulated using higher values similar to those which apply in real natural aspirated diesel engines. The basic conditions taken for the study are shown in *table II*.

TABLE II
Basic settings for the simulation.

| | |
|---|---|
| Initial pressure (MPa) | 3 |
| Initial temperature (K) | 800 |
| Partial pressure of NG (MPa) | 0.2 |
| Number of nozzle holes | 4 |
| Nozzle hole diameter (mm) | 0.2 |
| Injected mass of diesel (mg) | 32.76 |
| Diesel injection pressure (MPa) | 30 |
| Diesel injection duration (ms) | 1.55 |

## 4.2. Effect of the pilot injection pressure

The effects were evaluated in the present study by examining four different injection pressures as shown in *table III*.

*Figure 4* shows pressure traces for different diesel fuel injection pressures. In all four cases during the early stages of combustion, the burning of the gaseous fuel is

TABLE III
Injection pressure settings.

| | Case K1 | Case K2 | Case K3 | Case K4 |
|---|---|---|---|---|
| Diesel injection pressure (MPa) | 120 | 60 | 30 | 20 |
| Diesel injected mass (mg) | 26.7 | 26.7 | 26.7 | 26.7 |
| Nozzle hole diameter (mm) | 0.123 | 0.148 | 0.178 | 0.2 |

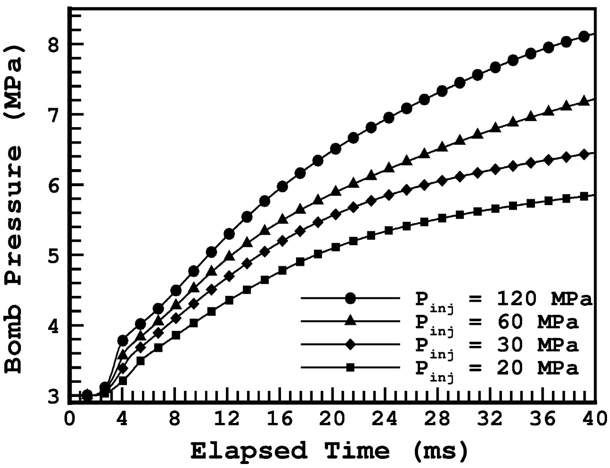


**Figure 4.** Effect of injection pressures on bomb combustion pressure partial pressure of natural gas: $P_{gas} = 0.2$ MPa.

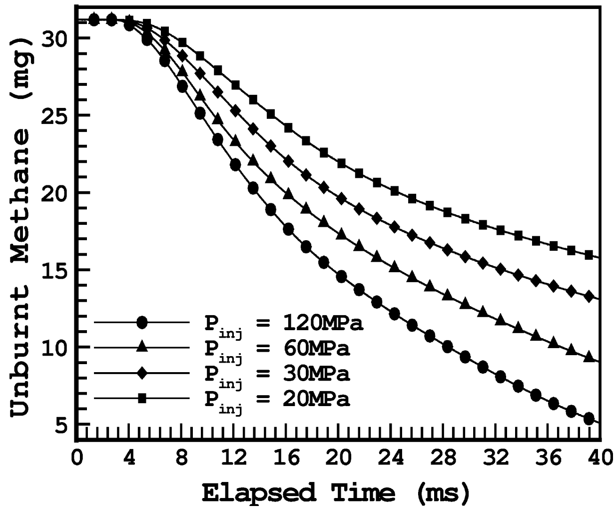


**Figure 5.** Effect of injection pressures on the mass of unburnt methane partial pressure of natural gas: $P_{gas} = 0.2$ MPa.

restricted to a small region near the injector. This is due to the high combustion temperature resulting from the initial, rapid combustion which tends to vaporise the fuel spray so quickly that the liquid fuel is unable to penetrate deeply into the combustion chamber. As the combustion continues, a slowly propagating flame front carries the combustion across the chamber. When the pilot-diesel injection pressure is increased from 20 MPa to 120 MPa, the rate of rise of the combustion pressure increases.

The methane starts to burn between 1 and 2 ms after the diesel fuel injection is completed. Following this, the flames from the various ignition centres originating from the pilot diesel fuel propagate throughout the chamber. As the pilot diesel pressure increases, the methane burns faster. As shown on *figure 5*, at a time of 40 ms, about 26 mg of methane (case K1) has burnt compared with the case K4, where only about 14 mg of methane has burnt. The reason is that, with greater pilot injection pressure, the outlet velocity and spray penetration have increased. This produces a larger quantity of well-mixed combustible gas before ignition consisting of the two fuels. As a result, the pilot fuel will burn faster which in turn will increase the activity of the partial oxidation reactions by increasing the overall temperature, thereby providing a larger combustion zone.

Spatial variations of gas temperatures are plotted at 16 ms after injection to examine the combustion and flame propagation through the air–NG mixture. These contours plots are drawn along the pilot distillate spray axis (*figure 6*). It can been seen that the flame propagates into the inner region of the diesel spray plume while simultaneously progressing outwards across the combustion chamber.

## 4.3. Effect of number of nozzle holes

Effects of number of injector nozzle holes on combustion were evaluated by investigating three different injectors with the same diesel mass flow rate. For this to be achieved, the nozzle hole diameters were reduced as their number increased. Three injector configurations were used with two, four, and eight holes respectively as shown on *table IV*.

TABLE IV
Nozzle parameter settings.

| | Case N1 | Case N2 | Case N3 |
|---|---|---|---|
| Number of nozzle holes | 2 | 4 | 8 |
| Nozzle hole diameter (mm) | 0.14 | 0.2 | 0.28 |
| Diesel injected mass (mg) | 32.76 | 32.76 | 32.76 |

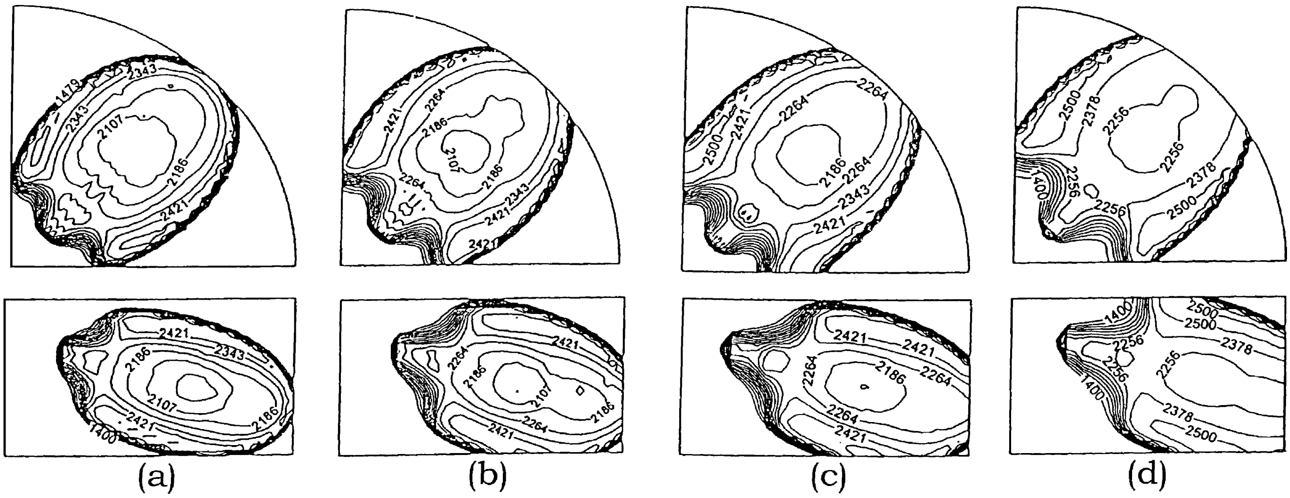


**Figure 6.** Contour plots of gas temperature at different injection pressures: (a) 20 MPa; (b) 30 MPa; (c) 60 MPa; (d) 120 MPa.

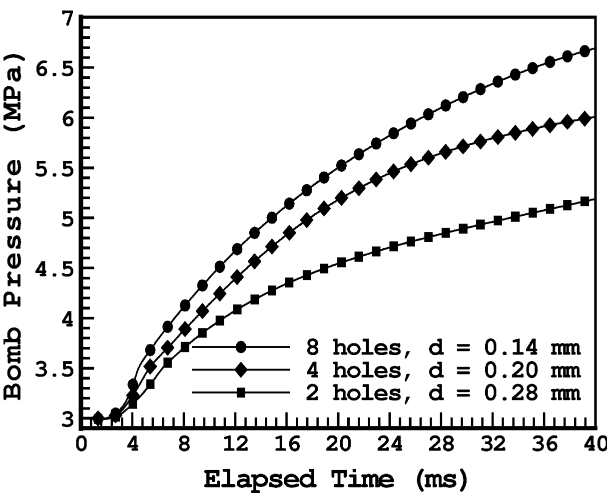


**Figure 7.** Effect of number of nozzle holes on bomb combustion pressure partial pressure of natural gas: $P_{gas} = 0.2$ MPa.

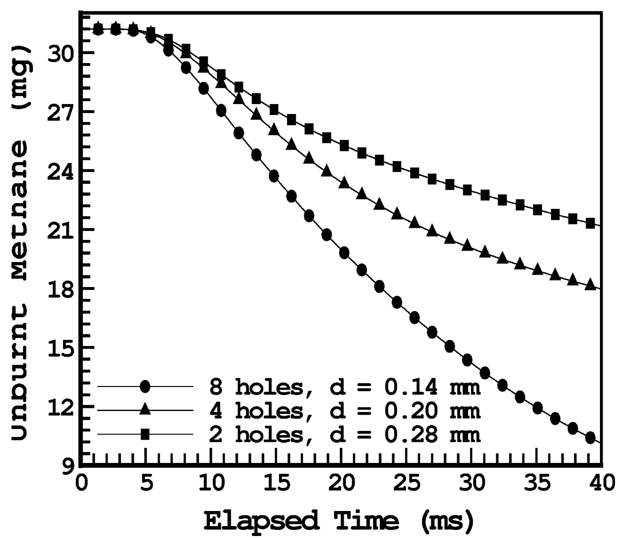


**Figure 8.** Effect of number of nozzle holes on the mass of unburnt methane partial pressure of natural gas: $P_{gas} = 0.2$ MPa.

The effect of the number of such nozzle holes on the combustion pressure is shown in *figure 7*. Only a small change, if any, occurs in the ignition delay. However, the overall effect is that the pressure rise rate is faster with an increasing number of holes. This is because more natural gas is ignited early in the combustion process.

As shown in *figure 8*, the mass of unburned methane reduces as the number of holes increases, a larger change occurring between 4 and 8 holes than between 2 and 4 holes. This shows improved early ignition of the gas phase occurs with more nozzle holes of smaller diameter.

In addition to the effects of pressure which is constant throughout the chamber at any one instant during combustion, it is again informative to examine properties that vary locally position. For this, the spatial variations of gas temperatures are plotted 8 ms after injection on *figure 9*. These contour plots are drawn along the pilot diesel spray axis. The differences in plots between the 8 hole nozzle, 4 hole nozzle and 2 holes nozzle are due to the change in symmetry for the simulation although all give comparable information. From these, it can been seen that while

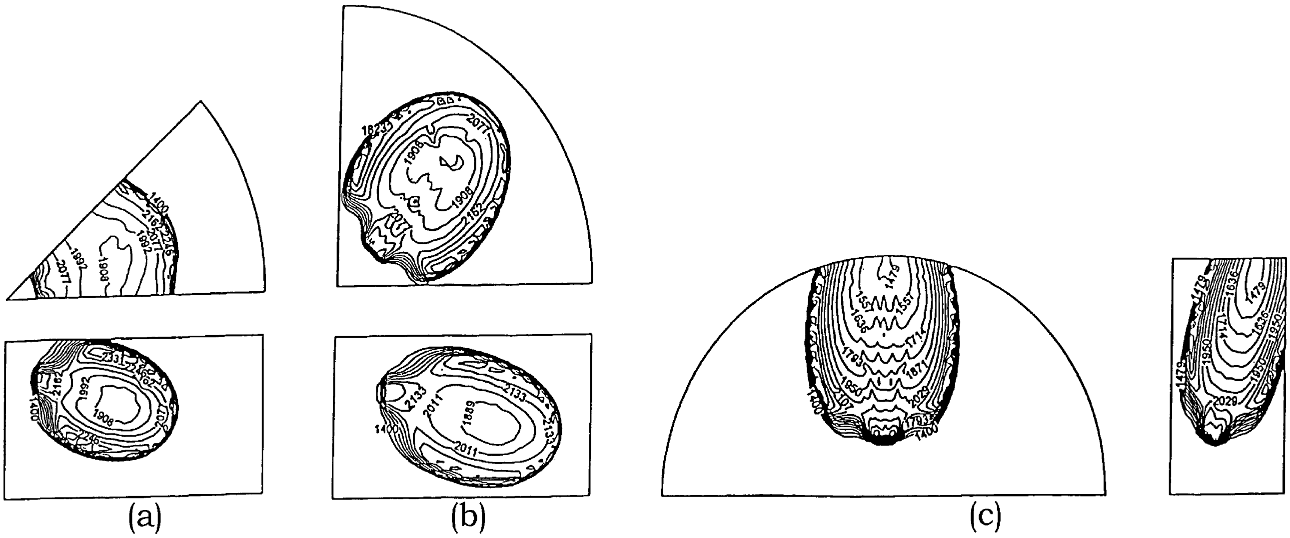

**Figure 9.** Contour plots of gas temperature for different number of nozzle holes: (a) 8 holes nozzle; (b) 4 holes nozzle; (c) 2 holes nozzle.

the radial penetration achieved by the flame is actually lower with more nozzle holes, the proportion of the volume engulfed by it is larger. That is, the basic effect is that each nozzle hole services a smaller volume of the chamber.

## 5. CONCLUSIONS

This study was undertaken to improve the understanding of how a pilot injection of diesel fuel affects the combustion of a natural gas–air mixture in an environment approximating that of a diesel cycle. After calibration of a 3D numerical model by combustion bomb tests, parametric studies were carried out which varied:

- the pilot injection pressures and
- the number and size of nozzles holes for a fixed diesel fuel flow rate.

Through an analysis of the combustion process, the following conclusions were reached:

(i) The numerical model gives a very good agreement with experimental results in predicating the combustion pressure. However, at the tail of the burning period, the experimental results fall more rapidly than do those of the simulation.

(ii) When the injection pressure increases from 20 MPa to 60 MPa, the combustion pressure increases by 30% at about 40 ms after injection. The higher fuel injection pressure gives a faster combustion of the natural gas. The results show that a high injection pressure has the beneficial effect of increasing the performance of dual fuel combustion.

(iii) For the same mass flow rate of diesel fuel, an increased number of holes of smaller diameter increases the early, premixed combustion due better fuel distribution and fuel vaporisation. The rate of burning of the natural gas is enhanced because the larger number of ignition centres from the pilot diesel fuel are distributed more widely throughout the chamber. As a result the performance of the dual fuel combustion improves.

## REFERENCES

[1] Nichols R.J., The challenges of change in the auto industry: why alternative fuels, J. Engrg. Gas Turbines Power 116 (4) (1994) 727–737.

[2] Karim G.A., A review of combustion process in the dual-fuel engine, Progr. Energy Combustion Sci. 6 (1980) 277–285.

[3] Karim G.A., Examination of the performance of a dual-fuel diesel engine with particular reference to the presence of some inert diluents in the engine intake charge, SAE Paper 821222, 1982.

[4] Karim G.A., Ignition of premixed gaseous fuel and air charge by pilot fuel spray injection with reference to dual-fuel combustion, SAE Paper 680768, 1968.

[5] Milton B.E., Improving the performance of small dual-fuelled engines, in: I$^{st}$ Natural Gas Vessel, Internat. Conference and Exhibition, Sydney, Australia, 1988, pp. 507–518.

[6] Karim G.A., Some measures towards enhancing the performance of methane fuelled diesel engines at light load, in: Internat. Conference and Exhibition, NGV '90, 1990, Paper No.59.

[7] Karim G.A., The dual-fuel engine of the compression ignition type-prospects, problems, and solutions—a review, SAE Paper 831073, 1983.

[8] Karim G.A., Knock in dual-fuel engines, Proc. Inst. Mech. Engrs. 181 (1(2)) (1966–1967) 435–466.

[9] Karim G.A., Burn K.S., The combustion of gaseous fuels in a dual-fuel engine of the compression ignition type with particular reference to cold intake temperature conditions, in: Proceeding of SAE Congress, February, 1980, Paper 800263.

[10] Karim G.A., Wiezaba P., Comparative studies of methane and propane as fuels for spark ignition and compression ignition engines, SAE Paper 831196, 1983.

[11] Mbarawa M., Problems related to the combustion of gaseous fuels (natural gas) in diesel engines, Ph.D. thesis, University of New South Wales, Australia, 1998.

[12] Choi I.S., Milton B.E., A dual-fuel combustion model for premixed natural gas with distillate ignition in a quiescent bomb, Numer. Heat Transfer, Internat. J. Computation Methodology, Part A: Applications 31 (7) (1997) 725–743.

[13] Launder B.E., Spalding D.B., The numerical computation of turbulent flows, Comput. Methods Appl. Mech. Engrg. 3 (1974) 269–289.

[14] Patankar S.V., Numerical Heat Transfer and Fluid Flow, Hemisphere, Washington, DC, 1980.

[15] Hiroyasu H., Nishida K., Fuel spray trajectory and dispersion in a direct injection diesel combustion chamber, SAE Paper 890462, 1989.

[16] Westbrook C.K., Dryer F.L., Simplified reaction mechanisms for the oxidation of hydrogen fuels in flames, Combustion Sci. Technology 27 (1981) 31–43.

[17] Olikara C., Borman G.L., A computer program for calculating properties for equilibrium combustion products with some applications to internal combustion Engines, SAE Paper 750468, 1975.

[18] Choi I.S., Milton B.E., Dual-fuel combustion with injected natural gas and distillate, in: Internat. Symposium on Advanced Computational Heat Transfer, Cesme, Turkey, 1997, pp. 75–82.

[19] Xu M., Nishida K., Hiroyasu H., A practical calculation method for injection pressure and spray penetration in diesel engines, SAE Paper 920624, 1992.